Spatial Formation Control with Volume Information: Application to Quadcopter UAV's ⋆

E.D. Ferreira-Vazquez [*] **E.G. Hernandez-Martinez** [**]
J.J. Flores-Godoy [***] **G. Fernandez-Anaya** [****]

[*] *Departamento de Ingeniería Eléctrica, Facultad de Ingeniería y Tecnologías, Universidad Católica del Uruguay, 11600, Montevideo, Uruguay (e-mail: enferrei@ucu.edu.uy).*
[**] *Departamento de Ingeniería, Universidad Iberoamericana, 01219, México City, México (e-mail: eduardo.gamaliel@ibero.mx).*
[***] *Departamento de Matemática, Facultad de Ingeniería y Tecnologías, Universidad Católica del Uruguay, 11600, Montevideo, Uruguay (e-mail: jose.flores@ucu.edu.uy).*
[****] *Depto. de Física y Matemáticas, Universidad Iberoamericana, 01219, México City, México (e-mail: guillermo.fernandez@ibero.mx).*

Abstract This paper extends the distance-based formation control for the case of holonomic robots moving in 3D space. The approach is addressed for agents modeled as double-integrators with any undirected communication graphs. The control strategy uses a combined distance-based attractive-repulsive potentials to ensure convergence to the formation pattern avoiding possible inter-robot collisions. In order to avoid unwanted formation patterns that verify the distance constraints, each robot control law includes a volume condition which provides information about the unique desired position of each robot in the formation pattern. The proposed algorithm is tested by numerical simulations and extended to the case of quadcopters UAV's by an input-output linearization showing good behavior.

Keywords: Mobile robots; Formation control; Artificial Potential Function; Collision Avoidance; Quadcopter UAV.

1. INTRODUCTION

Distance-based formation control (DFC) is a fundamental issue in the motion coordination of multi-robot systems (Oh et al., 2015). The main challenge is to design decentralized control strategies to move the robots to a desired formation pattern defined by distance constraints, avoiding inter-robot collisions. The control strategies encompass from reactive algorithms based in natural-behaviors (Yu and LaValle, 2012) to the use of communication graphs and distance-based functions with attractive and repulsive behavior in Dimarogonas and Johansson (2008).

The main drawback of the DFC with respect to the traditional position-based formation control widely studied in (Ren and Beard, 2008) and (Hernandez-Martinez and Aranda-Bricaire, 2011) falls in the generation of different final configurations of robots that satisfy the distance constraints.Therefore, rigidity problems arise (Krick et al., 2009). In this sense, a possible solution to achieve an unique formation pattern is to construct rigid patterns where at least $(n-3)$ communication edges for n robots must be defined as shown in (Olfati-Saber and Murray, 2002; Krick et al., 2008). Other approaches use additional information in the formation setup, such as absolute angle respect to a leader (Desai et al., 2001) or internal angles as studied in a previous work in (Ferreira-Vazquez et al., 2015).

Most of the DFC approaches have been addressed for the case of single-integrators robots moving in the plane, like in Dimarogonas and Johansson (2008) for the case of tree-shaped formations, DFC with cycles in (Dimarogonas and Johansson, 2009) or specific leader-followers schemes focus in the application to wheeled mobile robots in (Desai et al., 2001; Toibero et al., 2008). Feedback linearization techniques have been used when robot kinematics are more complex in (Liu and Jiang, 2013). The convergence of formations with mismatched distance constraints between agents is addressed in (Helmke et al., 2014). The DFC applied to the case of double-integrators is studied in Dimarogonas and Johansson (2008); Anderson et al. (2012) for the leader-followers scheme and Oh and Ahn (2014) for the case of undirected communication graphs using a gradient-like control law.

The extension to the case of agents moving in 3D space allows the application to formations of UAV's. Position-based formation control of quadcopters is studied in Alfriend et al. (2010); Sumano et al. (2013) using a reduce model of the position dynamics. Sliding mode control combined with neural networks is proposed in Bo and Gao (2009). The leader-follower scheme of distance and relative angle in UAV's is proposed in (Guangyan and Zheng, 2014) where an elastic term is added providing a better control effect. Collision avoidance of formation using Model Predictive Control (MPC) in discrete-time is given in (Chao et al., 2011), where the robots are formed with respect to a reference point. Finally, in

(Nielsen and Sharma, 2015) a DFC scheme is designed using the Lyapunov method, where the each robot keeps the leader vehicle at a desired bearing angle in its field-of-view using a video camera. In all the previous works, it is supposed an inner control related to the orientation angles of UAV's and the reduction of the position dynamics as a unicycle-type robot moving in a plane.

In this paper, we extend our previous work in (Ferreira-Vazquez et al., 2015) for the case of *3D* for spacial DFC and double integrator models, different to the absolute position-based formation in (Alfriend et al., 2010; Sumano et al., 2013). The formation strategy is based on artificial potential functions with attractive-repulsive behavior combined with information about the position of each robot respect to other three robots using a triple product. To the best of our knowledge, the triple product artificial potential has not been used in other works. The previous condition ensures the convergence to a unique formation pattern. The approach is applied to the case of quadcopter UAV's formations using input-output feedback linearization previously proposed in (Hernandez-Martinez et al., 2015), avoiding a model reduction of the orientational or translational dynamics as presented in (Guangyan and Zheng, 2014). Thus, the control approach becomes decentralized where the UAV's require to sense the displacement coordinates respect to its adjacent members defined by any well-defined and rigid undirected communication graph, becoming a more general result than the leader-follower setups given in (Bo and Gao, 2009; Chao et al., 2011). Simulations for the case of four UAV's with a virtual reality environment show the feasibility of the approach.

The paper is organized as follows. Section 2 formulates the formation problem. In Section 3, the control strategy is presented and the convergence is analyzed by Lyapunov techniques. Section 4 extends the result to the case of quadcopter UAV's with numerical simulations. Finally, section 5 presents some conclusion remarks and future work.

2. PROBLEM DEFINITION

2.1 Modified distance-based Formation Problem

Let $\mathbf{q} = [\mathbf{q}_1, \ldots, \mathbf{q}_N]^\top \in \mathbb{R}^{3 \times N}$ be the position of the center of N three-dimensional omnidirectional robots of diameter ρ_i with the double integrator dynamics given by the following equation:

$$\begin{aligned} \dot{\mathbf{q}}_i &= \mathbf{p}_i, \\ \dot{\mathbf{p}}_i &= \mathbf{u}_i, \end{aligned} \quad i = 1, \ldots, N \tag{1}$$

Let $\mathbf{r}_{ij} = \mathbf{q}_j - \mathbf{q}_i$ be the relative position vector of robot R_j with respect to robot R_i and

$$r_{ij} = \|\mathbf{r}_{ij}\| \tag{2}$$

be the Euclidean distance between robots R_i and R_j. A distance topology is defined by the sets $N_i, i = 1, \ldots, N$ of robot indexes j for which a desired distance d_{ij} between robots R_j and R_i is defined. It is assumed the topology is bidirectional, i.e. that $j \in N_i \implies i \in N_j$.

For any 4-tuple (i, j, k, m) the 3-simplex oriented volume define by robots R_i, R_j, R_k and R_m (Boyd and Vandenberghe, 2004) can be expressed by

$$\alpha_{ijkm} = \frac{1}{6} \mathbf{r}_{ij}^\top (\mathbf{r}_{ik} \times \mathbf{r}_{im}). \tag{3}$$

Figure 1 shows a representation of α_{ijkm} in space. This volume provides relative angular information between robots
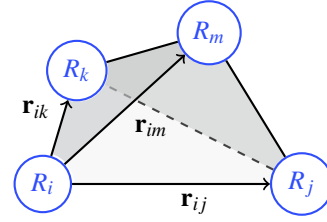

Figure 1. The value of α_{ijkm} is proportional to the tetrahedron volume enclosed by the robots R_i, R_j, R_k and R_m positions.
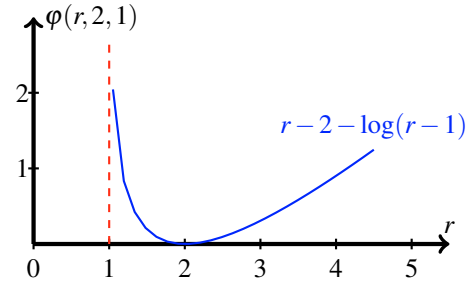

Figure 2. Combined attractive-repulsive artificial potential field as a function of r for the case where $d_{ij} = 2$ and $c_{ij} = 1$.

in a configuration $\mathbf{q}$. Let M be the set of all 4-tuples $(i_s, j_s, k_s, m_s), s = 1, \ldots, L$, for which a desired simplex volume $\alpha_{i_s j_s k_s m_s}^\star$ is defined. Taking into account the set M, a more restricted distance-based problem may be formulated as the following:

Problem Statement 1. Given N robots with dynamics defined by (1), find a control law for $\mathbf{u}_i, \forall i$ such that the robots converge without collisions to a configuration $\mathbf{q}$ verifying distance constraints $r_{ij} = d_{ij}, \forall j \in N_i$ and volume constraints $\alpha_{ijkm} = \alpha_{ijkm}^\star, \forall (i, j, k, m) \in M$.

A formulation to solve this problem is presented next.

3. FORMATION CONTROL

3.1 Combined attractive-repulsive artificial potential field

In order to converge to pre-specified inter-robot distances without collisions, an attractive-repulsive artificial potential field is used, given by the following definition.

Definition 1. Given any two robots R_i and R_j an Artificial Potential Field φ_{ij} is defined as:

$$\varphi_{ij}(r_{ij}, d_{ij}, c_{ij}) = \frac{r_{ij} - d_{ij}}{d_{ij} - c_{ij}} - \log\left(\frac{r_{ij} - c_{ij}}{d_{ij} - c_{ij}}\right) \tag{4}$$

with r_{ij} given by (2), d_{ij} their desired distance and

$$c_{ij} = \frac{1}{2}(\rho_i + \rho_j) \tag{5}$$

their collision distance where ρ_k, $k = 1, \ldots, N$ the robot diameters and $d_{ij} > c_{ij}$.

Figure 2 shows the shape of the combined potential field. Observe also that φ_{ij} is well defined for $r_{ij} > c_{ij}$ and tends to $+\infty$ when $r_{ij} \to c_{ij}$ with $r_{ij} > c_{ij}$.

3.2 Repulsive potential field

In a general formation specification there will be robots that do not communicate with each other due to several reasons. For

those cases, there should still exist a repulsive action to prevent collisions. Therefore, a repulsive artificial potential field is defined as follows.

Definition 2. Given two robots located at $\mathbf{q}_i$ and $\mathbf{q}_j$ with $j \notin N_i$, an Artificial Repulsive Potential Field χ_{ij} is defined as:

$$\chi_{ij} = \begin{cases} 0, & r_{ij} > D_{ij} \\ \dfrac{r_{ij} - D_{ij}}{D_{ij} - c_{ij}} - \log\left(\dfrac{r_{ij} - c_{ij}}{D_{ij} - c_{ij}}\right) & r_{ij} < D_{ij} \end{cases} \tag{6}$$

with r_{ij} given by (2), D_{ij} the range of the repulsive potential and c_{ij} given by (5).

It is assumed that the range of the sensor is greater than the collision distance, therefore $D_{ij} > c_{ij}$, $\forall i, j$ and the potential χ_{ij} is well defined.

3.3 Artificial volume potential field

The following potential field uses volume information given by coefficients α_{ijkm} to help drive the robots to a configuration $\mathbf{q}$ with specific values of α_{ijkm}, $\forall (ijkm) \in M$.

Definition 3. Given any four different robots R_i, R_j, R_k and R_m located at $\mathbf{q}_i$, $\mathbf{q}_j$, $\mathbf{q}_k$ and $\mathbf{q}_m$ respectively, an artificial volume potential field ψ_{ijkm} is defined as:

$$\psi_{ijkm}(\theta, \eta) = \kappa(\theta \alpha^\star_{ijkm} - \eta \alpha_{ijkm}) \tag{7}$$

with $\theta > 0$, α_{ijkm} is the 3-simplex volume defined in (3) and $\alpha^\star_{ijkm}$ its desired value. The function $\kappa : \mathbb{R} \to \mathbb{R}$ satisfies the following conditions:

(1) κ is differentiable with continuous first derivative in $\mathbb{R}$.
(2) $\kappa(x) = 0, \forall x \le 0$.
(3) $\kappa(x) > 0$ and nondecreasing $\forall x > 0$.

3.4 Formation Control Strategy

This section states the main result, i.e. a control approach that uses relative volume information between robots to achieve a desired configuration satisfying distance and volume constraints.

Theorem 1. Given N sphere-sized robots $R_i, i = 1, \ldots, N$ with positions and diameters given by $\mathbf{q}_i$ and ρ_i respectively, dynamics defined by (1), bidirectional distance topology defined by the sets N_i and volume topology set M. For the case of the Problem Statement 1, with a desired rigid configuration specified by distances d_{ij} $\forall j \in N_i$ and compatible volume constraints given by the set $\Gamma^\star = \{\alpha^\star_{ijkm}, \forall (i, j, k, m) \in M\}$, the following control law:

$$\mathbf{u}_i = -K_d \nabla_i \varphi_i - K_r \nabla_i \chi_i - K_v \nabla_i \psi^\star - K_p \mathbf{p}_i \tag{8}$$

$$\varphi_i = \sum_{j \in N_i} \varphi_{ij} \tag{9}$$

$$\chi_i = \sum_{j \notin N_i} \chi_{ij} \tag{10}$$

$$\psi^\star = \sum_{\substack{i,j,k,m \\ (i,j,k,m) \in M}} \psi^\star_{ijkm} \tag{11}$$

$$\psi^\star_{ijkm} = \psi_{ijkm}(\alpha^\star_{ijkm}, \alpha^\star_{ijkm}) \tag{12}$$

with φ_{ij} the combined attractive-repulsive artificial potential field defined by (4), χ_{ij} a repulsive artificial potential field to be used between robots that are not communicated to each other defined by (6), and ψ_{ijkm} the artificial volume potential field defined by (7) and positive control parameters K_d, K_r, K_v and

K_p will drive the robots without collisions to a configuration where all robots stop.

Proof. Let $\Phi^\star$ be the set of all robot configurations $\mathbf{q}^\star$ verifying the distance and volume constraints. It is assumed that the constraints are suitable such that $\Phi^\star \neq \varnothing$. Define a Lyapunov function candidate $V_A(\mathbf{q})$ as,

$$V_A(\mathbf{q}) = \lambda_d \sum_{i=1}^N \varphi_i + \lambda_r \sum_{i=1}^N \chi_i + \lambda_v \psi^\star + \sum_{i=1}^N \mathbf{p}_i^\top \mathbf{p}_i, \tag{13}$$

with λ_d, λ_r and λ_v positive constants to be defined later. Since all artificial potential fields φ_{ij}, χ_{ij} and $\psi^\star$ are positive semidefinite functions by definition it follows that:

$$V_A(\mathbf{q}) = 0, \quad \forall \mathbf{q} \in \Phi^\star$$
$$V_A(\mathbf{q}) > 0, \quad \forall \mathbf{q} \notin \Phi^\star$$

Evaluating the time derivative of V_A along the trajectories of the system (1),

$$\dot{V}_A(\mathbf{q}) = \lambda_d \sum_i \dot\varphi_i + \lambda_r \sum_i \dot\chi_i + \lambda_v \dot\psi^\star + \sum_i \mathbf{p}_i^\top \dot{\mathbf{p}}_i$$
$$= \sum_l \sum_i \nabla_l^\top (\lambda_d \varphi_i + \lambda_r \chi_i) \mathbf{p}_l + \sum_l \lambda_v \nabla_l^\top \psi^\star + \sum_i \mathbf{p}_i^\top \dot{\mathbf{p}}_i \tag{14}$$

By substituting equations (9) and (11) into (14), the time derivative of the Lyapunov function transforms into,

$$\dot{V}_A(\mathbf{q}) = \sum_{l,i} \nabla_l^\top \left(\lambda_d \sum_{j \in N_i} \varphi_{ij} + \lambda_r \sum_{j \notin N_i} \chi_{ij} \right) \mathbf{p}_l$$
$$+ \lambda_v \sum_l \nabla_l^\top \psi^\star \mathbf{p}_l + \sum_l \mathbf{p}_l^\top \mathbf{u}_l \tag{15}$$

Taking the gradients of the potential fields from equations (4) and (6) and using their symmetric properties and bidirectionality of the distance topology it follows that (Ferreira-Vazquez et al., 2015)

$$\dot{V}_A(\mathbf{q}) = 2 \sum_l \nabla_l^\top (\lambda_d \varphi_l + \lambda_r \chi_l) \mathbf{p}_l$$
$$+ \lambda_s \sum_l \nabla_l^\top \psi^\star \mathbf{p}_l + \lambda_v \sum_l \mathbf{p}_l^\top \mathbf{u}_l \tag{16}$$

Substituting the control action (8) gives

$$\dot{V}_A(\mathbf{q}) = \sum_l \nabla_l^\top ((2\lambda_d - K_d)\varphi_l + (2\lambda_r - K_r)\chi_l) \mathbf{p}_l$$
$$+ (\lambda_v - K_v) \sum_l \nabla_l^\top \psi^\star \mathbf{p}_l - K_p \sum_l \mathbf{p}_l^\top \mathbf{p}_l \tag{17}$$

Choosing $2\lambda_d = K_d$, $2\lambda_r = K_r$ and $\lambda_v = K_v$, equation (16) becomes

$$\dot{V}_A(\mathbf{q}) = -K_p \sum_l \mathbf{p}_l^\top \mathbf{p}_l \le 0 \tag{18}$$

Using Lasalle's invariant principle, the system will converge to the largest invariant set $\mathbb{M}$ for which $\dot{V}_A(\mathbf{q}) = 0 \implies \mathbf{p}_i = 0, \forall i$. Applying Barbalat's lemma implies $\dot{\mathbf{p}}_i = \mathbf{u}_i \to 0$ which gives the conditions

$$\mathbf{p}_i = 0,$$
$$K_d \nabla_i \varphi_i - K_r \nabla_i \chi_i - K_v \nabla_i \psi^\star = 0, \quad \forall i = 1, \ldots, N. \tag{19}$$

Besides, assuming the robots are not colliding initially $V_A(\mathbf{q})$ is bounded from above at $t = 0$ and will remain bounded for all $t > 0$. Therefore, the robot trajectories do not collide.

It should be observed that equations (19) imply that all robots stop. It is clear by definition that $\Phi^\star \subseteq \mathbb{M}$. Besides, configurations that satisfy distance constraints d_{ij} but have

opposite values of $\alpha^\star_{ijkm}$ which are generated by plane symmetries, are not equilibrium states anymore. However, there may still be unwanted local minima inside $\mathbb{M}$. Nevertheless, by using larger values of λ_v, i.e. larger values of K_v, the regions of attraction of those local equilibrium states are being reduced with respect to the desired final state. ∎

From a practical implementation standpoint, taking the gradient of the volume potential (7) gives

$$\nabla_l \psi^\star_{ijkm} = \frac{d\kappa}{dx} \alpha^\star_{ijkm} \left(\delta_{li} \mathbf{r}_{jk} \times \mathbf{r}_{km} + \delta_{lj} \mathbf{r}_{km} \times \mathbf{r}_{mi} \right. \\ \left. + \delta_{lk} \mathbf{r}_{mi} \times \mathbf{r}_{ij} + \delta_{lm} \mathbf{r}_{ij} \times \mathbf{r}_{jk} \right) \quad (20)$$

with δ_{ab} the Kronecker's delta function. Each robot in the 4-tuple will implement one and only one of the terms on the right hand side of (20) and they only need local information of distances and angles to compute it. Besides, in the case of a desired rigid configuration $\mathbf{q}^\star$, only the signs of $\alpha^\star_{ijkm}$ are needed in the proof to have convergence.

4. EXTENSION TO THE CASE OF QUADCOPTER UAV'S

In this Section, the DFC obtained for the general case of robots moving in the space is extended to the case of Quadcopter UAV's formations. According to the Fig. 3 and recalling our previous work given in (Hernandez-Martinez et al., 2015), consider the coordinates of position $\xi = [x, y, z]^T$ and orientation $\eta = [\phi, \theta, \psi]^T$ (roll, pitch and yaw, respectively) of the body frame Γ_b respect to fixed frame Γ_e. Then, the translational and rotational dynamical model of the quadcopter UAV can be obtained as

$$m\ddot{\xi} = R^e_b \begin{bmatrix} 0 \\ 0 \\ F \end{bmatrix} + \begin{bmatrix} 0 \\ 0 \\ -mg \end{bmatrix} \quad (21)$$

$$\widetilde{J}\ddot{\eta} = \tau - C(\eta, \dot{\eta})\dot{\eta} \quad (22)$$

where m is the mass of the vehicle, g is the gravitational constant, F is the main thrust force applied in the center of mass, R^e_b is the result of the multiplication of the three standard rotations matrices, that results in

$$R^e_b = \begin{bmatrix} c\psi c\theta & -c\theta s\psi & s\theta \\ c\phi s\psi + c\psi s\phi s\theta & c\phi c\psi - s\phi s\psi s\theta & -c\theta s\phi \\ s\phi s\psi - c\phi c\psi s\theta & c\psi s\phi + c\phi s\psi s\theta & c\phi c\theta \end{bmatrix} \quad (23)$$

with $c\phi = \cos\phi$, $c\theta = \cos\theta$, $c\psi = \cos\psi$ and $s\phi = \sin\phi$, $s\theta = \sin\theta$, $s\psi = \sin\psi$. On the other hand, $\widetilde{J} = JW_n$ and $C(\eta, \dot{\eta}) = J\dot{W}_n$ is the Coriolis term with J the inertial symmetrical matrix and

$$W_n = \begin{bmatrix} 1 & 0 & -\sin\theta \\ 0 & \cos\phi & \cos\theta \sin\phi \\ 0 & -\sin\phi & \cos\theta \cos\phi \end{bmatrix} \quad (24)$$

and finally, $\tau = [\tau_\phi, \tau_\theta, \tau_\psi]^T$ are the torques generated by the rotors in Γ_b. According to the position and turning sense of the rotors given in the Fig. 3, the F and τ control inputs are obtained through

$$\begin{bmatrix} F \\ \tau \end{bmatrix} = \begin{bmatrix} 1 & 1 & 1 & 1 \\ -\ell & \ell & 0 & 0 \\ 1 & 0 & -\ell & \ell \\ -\dfrac{b}{k} & -\dfrac{b}{k} & \dfrac{b}{k} & \dfrac{b}{k} \end{bmatrix} \begin{bmatrix} f_1 \\ f_2 \\ f_3 \\ f_4 \end{bmatrix} \quad (25)$$

where ℓ be the length of every arm of the quadcopter, b is the drag constant and $f_i = k\omega_i^2$, $i = 1, ..., 4$ are the indivual thrust
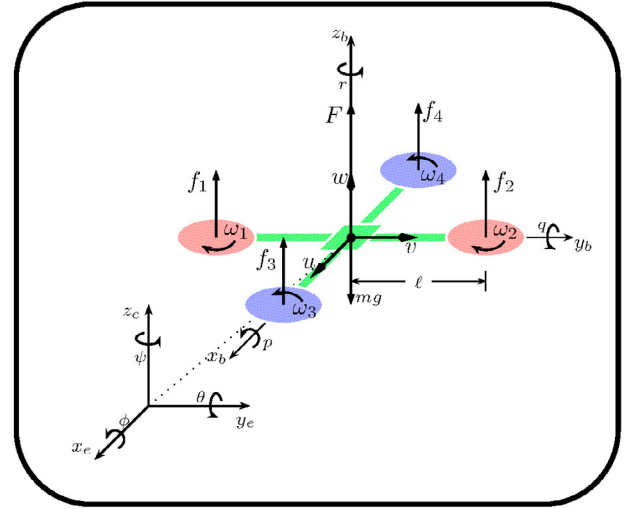

Figure 3. Quadcopter configuration scheme

forces of each rotor, where k is the thrust constant and ω_i are the angular velocities.

Substituting the rotational matrix R^e_b given in (23) and defining a control law $\tau = \widetilde{J}\widetilde{\tau} + C(\eta, \dot{\eta})\dot{\eta}$, where $\widetilde{\tau} = [\widetilde{\tau}_\phi, \widetilde{\tau}_\theta, \widetilde{\tau}_\psi]^T$ constitutes the vector of auxiliar torques, the dynamical system (21-22) results in

$$m\ddot{\xi} = \begin{bmatrix} F\sin\theta \\ -F\cos\theta\sin\phi \\ F\cos\theta\cos\phi - mg \end{bmatrix} \quad (26)$$

$$\ddot{\eta} = \widetilde{\tau} \quad (27)$$

According to (Hernandez-Martinez et al., 2015), the quadcopter control can be decomposed in two hierarchical levels (posture control and orientation control) assuming that the rotational dynamics converges faster than the translational dynamics. Thus, the translational dynamics (26), considering as control inputs to F, θ and ϕ (note that ψ is not required), can be input-output linearized by the control laws

$$\theta_d = \arctan\left(\frac{u_x \cos\phi}{u_z + g} \right),$$

$$\phi_d = \arctan\left(-\frac{u_y}{u_z + g} \right) \quad (28)$$

$$F = \frac{m(u_z + g)}{\cos\theta \cos\phi}$$

where $u = [u_x, u_y, u_z]^T$ are the auxiliary translational control inputs for the three axis. On the other hand, for the dynamics of the orientation angles (27), the inner loop generates the desired values of the orientation angles using the control laws

$$\widetilde{\tau} = \ddot{\eta}_d - \gamma_2(\dot{\eta} - \dot{\eta}_d) - \gamma_1(\eta - \eta_d) \quad (29)$$

where $\gamma_1, \gamma_2 > 0$ are control parameters and $\eta_d = [\phi_d, \theta_d, \psi_d]^T$, where ψ_d constitutes the (independent) function of the yaw angle. Note that substituting (29) in (27), a linear equation of the angle errors given by $e_\eta = \eta - \eta_d$ is obtained. Note that an appropriate selection of control gains and initial conditions can ensure small values of the orientation angles, avoiding the indetermination of the control laws (28). It is important to ensure a fast convergence of the orientation angles respect to the translational coordinates.

Finally, applying the control laws (28) and (29), the quadcopter UAV is viewed in the translational dynamics as a double integrator agent given by $\ddot{\xi} = u$. If we consider a set of n quadcopter UAV's, then the dynamical systems can be written as

$$\ddot{\xi}_i = u_i, i = 1, ..., n \qquad (30)$$

which falls in the case of omnidirectional agents addressed in the previous case.

4.1 Numerical simulation of DFC of Quadcopter UAV's

The results of a numerical simulation of the DFC applied to a four quadcopter UAV's are presented in Figures 4 to 8 with the following parameters. The initial position of the coordinates ξ_i, $i = 1, ..., 4$ of the robots are given by $\xi_1(0) = [10, 0, 5]^T$, $\xi_2(0) = [-5, -10, 3]^T$, $\xi_3(0) = [10, -5, 10]^T$ and $\xi_4(0) = [10, -10, 10]^T$. The desired distances between robots is given by $d_{ij} = 5$ and the collision distance is given by $c_{ij} = 3.5$, $\forall i, j \in N, i \neq j$. For of each quadcopter $m_i = 1$ kg; $\ell_i = 0.3$ m; $b_i = 0.001$ m^{2}kg; $k_i = 0.0005$ kg m $\forall i$, $i = 1, 2, 3, 4$. For the volume constraints the value selected was $\alpha^\star_{1234} = -1$, $\alpha^\star_{2341} = 1$, $\alpha^\star_{3412} = -1$, $\alpha^\star_{4123} = 1$. There is complete communication topology between all robots therefore the repulsive artificial potential field of (6) is not necessary and $K_r = 0$. The value for the gains associated with the consensus control law given in Theorem 1 are $K_d = 0.1$, $K_v = 0.2$, $K_p = 1$. Note that the robots converge to their desired inter-agents distances, as shown in Figure 4 achieving a tetrahedron-shape formation. This is shown in Figure 5, where distances r_{ij} between robots R_i and R_j converge to 5 $\forall i, j$. Also, the volume constraints $\alpha^\star_{ijkm}$ are satisfied. Figure 6 shows the control inputs generated by the DFC law given by (8). With the control input (8) we can produce the desired angles and main thrust forces for each quadcopter UAV given by (28) also with the inner loop control given by (29), with $\gamma_1 = 1.8598$ and $\gamma_2 = 6.9177$, and $\psi_d = 0$ we can compute the orientation angles for the quadcopters and are shown in Figure 7 and Figure 8. Observe that the orientation angles converge to their desired valued and also the main thrust force converges to a constant value which indicates that the quadcopters are in hoover mode preserving the desired formation. In order to show the robustness of the approach, a pulse perturbation is added in the control input U_1 at the time instant $t = 150$ with amplitude 0.01 and duration of 0.1 seconds. Also a band-limited white noise with a power noise of 0.0001 is added to the quadcopter UAV 4 at $t = 200$. Note that the performance of all signals is acceptable remaining in a neighborhood of their desired values.

5. CONCLUSIONS

This work presents a formulation for a spatial distance based formation control of groups of 3D double integrator agents with any undirected communication graphs. The approach uses a combined attractive-repulsive artificial potential field and a novel control term related to a volume condition which provides information about the unique desired position of each robot in the formation pattern. This volume condition constraints the position of a robot with respect to a virtual plane described by three other robots. With this strategy it is possible to avoid unwanted formation patterns that verify the same distance restrictions. The control law is extended to the case of nonholonomic robots such as quadcopters UAV.
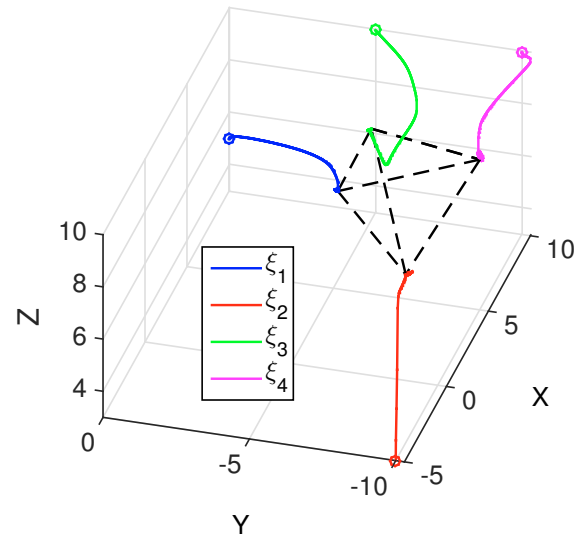

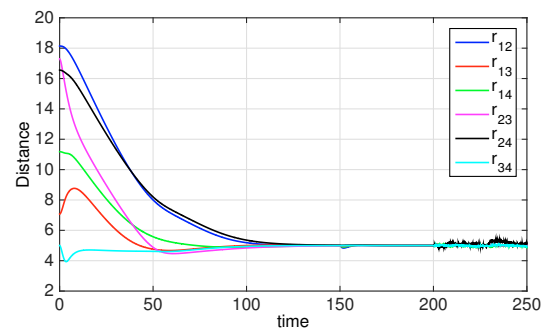Figure 4. Trajectories of quadcopters in the space
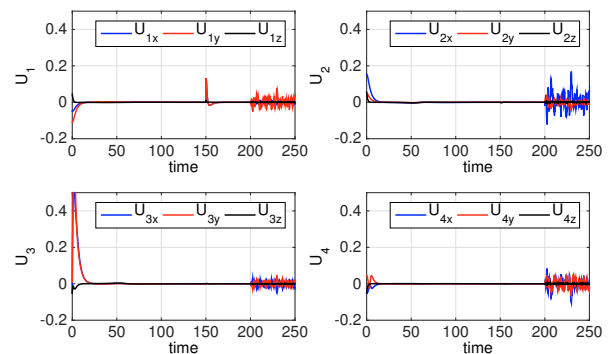

Figure 5. Distances between quadcopters

Figure 6. Control inputs of the formation strategy

Even though the quadcopter control law separates the control objective in two different loops—translational and rotational loops—the numerical simulation shows that the DFC achieves its objective of convergence to a desired inter-robot distance. As a future work the DFC control laws will be implemented with a real setup of quadcopters and the possibility to extend the strategy to solve the problem of flocking behavior. Also some other communication topologies need to be investigated.
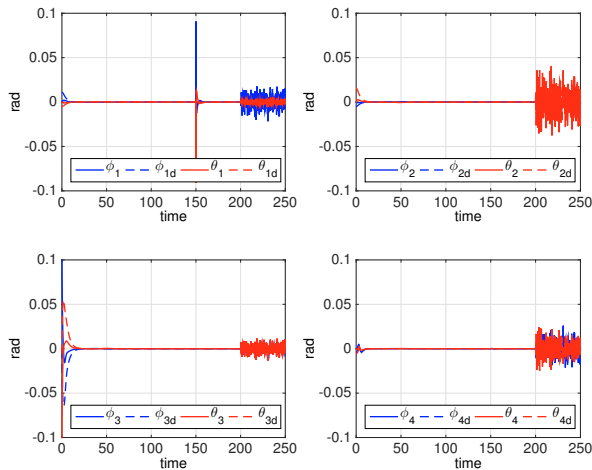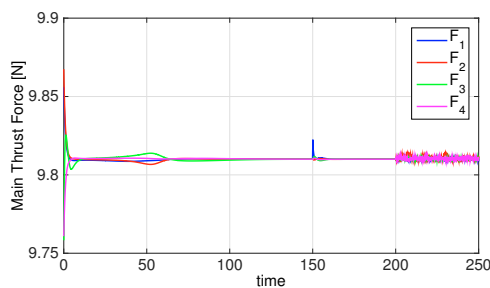
Figure 7. Trajectories of the orientation angles

Figure 8. Trajectories of main thrust forces

REFERENCES

Alfriend, K.T., Vadali, S.R., Gurfil, P., How, J.P., and Breger, L.S. (2010). *Spacecraft formation flying : dynamics, control, and navigation*. Butterworth-Heinemann, Oxford.

Anderson, B., Lin, Z., and Deghat, M. (2012). Combining distance-based formation shape control with formation translation. In L. Qiu, J. Chen, T. Iwasaki, and H. Fujioka (eds.), *New Trends in Control and Networked Dynamical Systems*, volume 1, 121–130. IET, 1st edition.

Bo, X. and Gao, Y. (2009). Sliding mode control of space robot formation flying. In G.S. Gupta and S.C. Mukhopadhyay (eds.), *4th International Conference on Autonomous Robots and Agents (ICARA)*, 561–565. IEEE.

Boyd, S. and Vandenberghe, L. (2004). *Convex Optimization*. Cambridge University Press, New York, NY, USA.

Chao, Z., Ming, L., Shaolei, Z., and Wenguang, Z. (2011). Collision-free uav formation flight control based on nonlinear mpc. In *International Conference on Electronics, Communications and Control (ICECC)*, 1951–1956.

Desai, J., Ostrowski, J.P., and Kumar, V. (2001). Modeling and control of formations of nonholonomic mobile robots. *Robotics and Automation, IEEE Transactions on*, 17(6), 905–908.

Dimarogonas, D.V. and Johansson, K.H. (2009). Further results on the stability of distance-based multi-robot formations. In *American Control Conference (ACC'09)*, 2972–2977. IEEE.

Dimarogonas, D.V. and Johansson, K.H. (2008). On the stability of distance-based formation control. In *47th IEEE/CDC Conference on Decision and Control*, 1200–1205. IEEE.

Ferreira-Vazquez, E., Hernandez-Martinez, E., Flores-Godoy, J., Fernandez-Anaya, G., and Paniagua-Contro, P. (2015). Distance-based Formation Control using Angular Information between Robots. *Journal of Intelligent and Robotic Systems*, 1(1), 1–18.

Guangyan, X. and Zheng, L. (2014). Distributed control of nonlinear elastic formation of unmanned aerial vehicles. In *IEEE Chinese Guidance, Navigation and Control Conference*, 2181–2186.

Helmke, U., Mou, S., Z., S., and Anderson, B. (2014). Geometrical methods for mismatched formation control. In *53rd IEEE Conference on Decision and Control*, 1341–1346.

Hernandez-Martinez, E.G. and Aranda-Bricaire, E. (2011). Convergence and collision avoidance in formation control: A survey of the artificial potential functions approach. In F. Alkhateeb, E.A. Maghayreh, and I.A. Doush (eds.), *Multi-agent systems—modeling, control, programming, simulations and applications*, 103–126. INTECH, Austria.

Hernandez-Martinez, E., Fernandez-Anaya, G., Ferreira-Vazquez, E., Flores-Godoy, J., and Lopez-Gonzalez, A. (2015). Trajectory tracking of a quadcopter uav with optimal translational control. In *11th IFAC Symposium on Robot Control*, 228–233.

Krick, L., Broucke, M., and Francis, B. (2008). Stabilization of infinitesimally rigid formations of multi-robot networks. In *IEEE Conference on Decision and Control*, 477–482.

Krick, L., Broucke, M.E., and Francis, B.A. (2009). Stabilisation of infinitesimally rigid formations of multi-robot networks. *International Journal of Control*, 82(3), 423–439.

Liu, T. and Jiang, Z.P. (2013). A nonlinear small-gain approach to distributed formation control of nonholonomic mobile robots. In *American Control Conference (ACC), 2013*, 3051–3056.

Nielsen, J. and Sharma, R. (2015). Formation control of quad-rotor uavs using a single camera. In *International Conference on Unmanned Aircraft Systems (ICUAS)*, 18–25.

Oh, K.K. and Ahn, H.S. (2014). Distance-based undirected formations of single-integrator and double-integrator modeled agents in n-dimensional space. *International Journal of Robust and Nonlinear Control*, 24(12), 1809–1820. doi:10.1002/rnc.2967. URL http://dx.doi.org/10.1002/rnc.2967.

Oh, K.K., Park, M.C., and Ahn, H.S. (2015). A survey of multi-agent formation control. *Automatica*, 53(0), 424 – 440.

Olfati-Saber, R. and Murray, R. (2002). Distributed cooperative control of multiple vehicle formations using structural potential functions. In *IFAC World Congress*, 346–352.

Ren, W. and Beard, R. (2008). *Distributed Consensus in Multi-vehicle Cooperative Control*. Springer, London.

Sumano, E., Castro, R., and Lozano, R. (2013). Sinchronization of quadrotors in coordinated manner (in spanish). In *Congreso Nacional de Control Automático 2013*, 1–6.

Toibero, J., Roberti, F., Fiorini, P., and Carelli, R. (2008). Hybrid formation control for non-holonomic wheeled mobile robots. In I.S. S. Lee and M. Ki (eds.), *Lecture Notes in Control and Information Sciences*, volume 370, 21–34. Springer, 1st edition.

Yu, J. and LaValle, S.M. (2012). Distance optimal formation control on graphs with a tight convergence time guarantee. In *IEEE Conference on Decision and Control*, 4023–4028.